SPECTROSCOPIC OBSERVATIONS OF ELECTRONIC STRUCTURES IN DENSE PLASMAS

Hyun-Kyung Chung
Gwangju Institute of Science and Technology (GIST)
Gwangju, Republic of Korea

Joint ICTP-IAEA School and Workshop on Fundamental Methods for Atomic, Molecular and Materials Properties in Plasma Environments
Trieste, Italy, 16-20 April 2018

OUTLINE

- Introduction
  - High Energy Density Physics
  - Extreme States of Matter produced in Laboratories
- Dense Plasmas Generated by X-Ray Free Electron Lasers
  - Atomic Processes in Extreme States of Matter
- Spectroscopic Observation of Electronic Structures
  - Ionization Potential Depression
  - Increased Collisional Ionization Rates
- Concluding Remarks

Matter under Extreme Conditions

Pressure conditions > 1 Mbar

HIGH ENERGY DENSITY PHYSICS

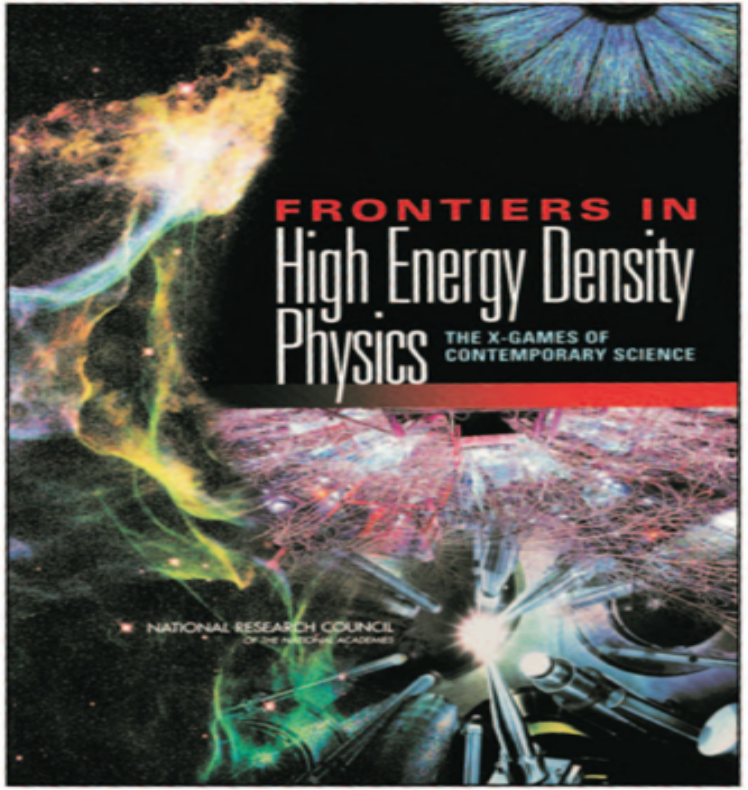

High Energy Density Physics: Studies of Matter under Extreme Conditions

- One of the “hottest” and most rapidly developing basic scientific disciplines.
- Interfaced between
  - Plasma physics
  - Nonlinear optics
  - Physics of lasers and charged-particle beams
  - Relativistic physics
  - Condensed-matter physics
  - Nuclear, Atomic and Molecular physics
  - Radiative, gas and magnetic hydrodynamics
  - Astrophysics
- Information about the thermodynamic, structural, gas-dynamic, optical, electro-physical and transport properties of matter under extreme conditions

Definition of High Energy Density (HED)

- Lowest bound of HED: external energy density comparable to the material's room temperature energy density
- The energy density of a hydrogen molecule and the bulk moduli of solid-state materials are similar about 10^{11}J/m^3 (The pressure is ~ 1 Mbar).

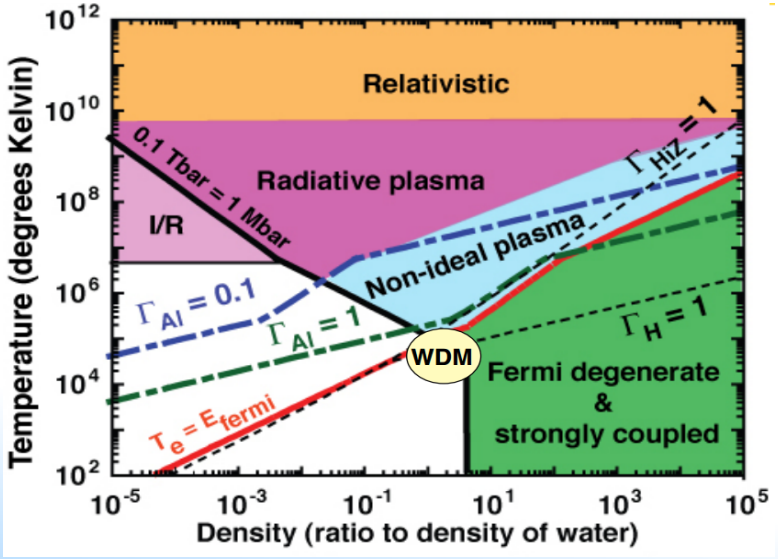

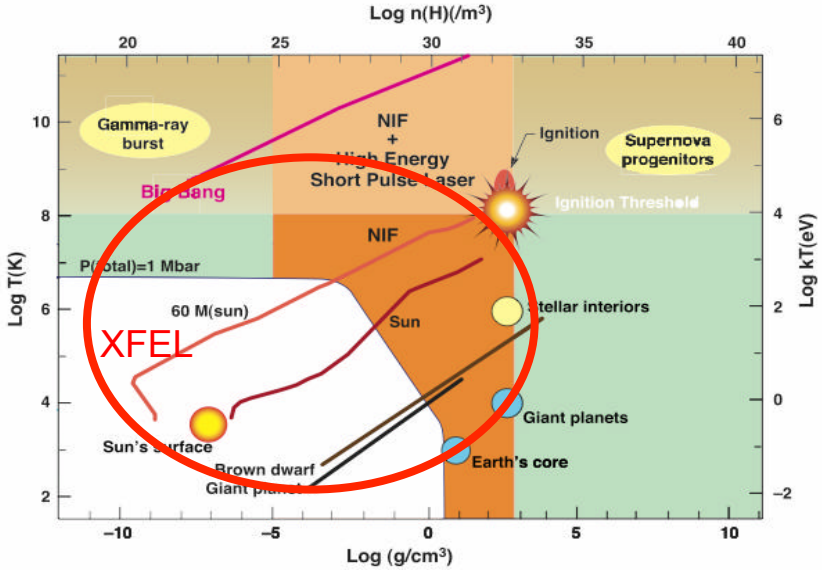

High Energy Lasers

National Ignition Facility (NIF) LLNL, USA (2010)

- 1.8 MJ 192 UV beam (4.2 MJ IR beam)
- 10^8 K, 100 times of lead density, 100 Mbar pressure
- 0.3 mm spot size, 1-20 ns, 2 x 10^{15} W/cm^2

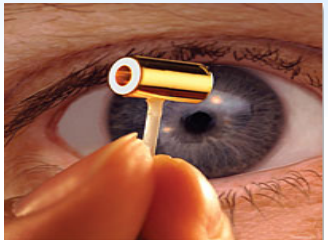

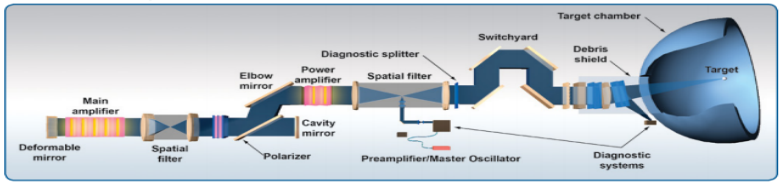

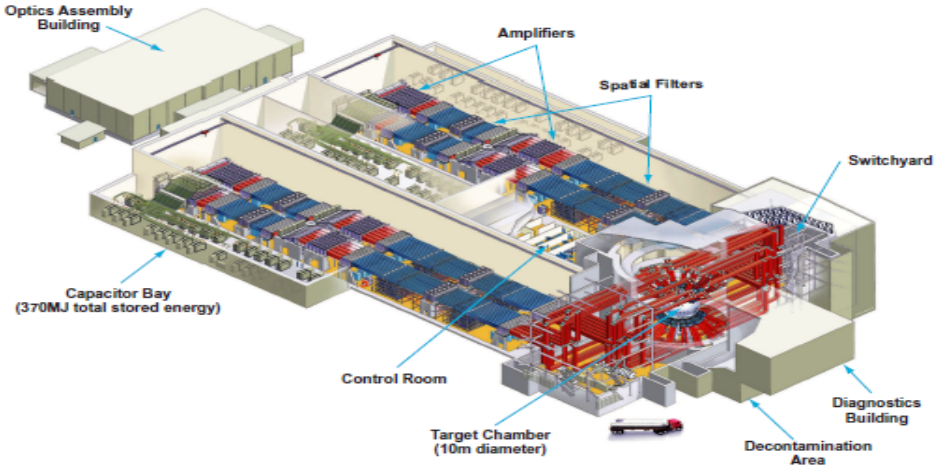

High Power Lasers

Extreme Light Infrastructure (ELI), Czech (2018)

- 0.2 EW (200 PW, 0.2×10^{18} W), 3-4 kJ, 15 fs
- Physics of vacuum in the presence of extremely high light fields
- Sources of accelerated charged particles and photons (300 Gbar for 10^{21}W/cm^2)
- Nuclear processes under super high laser fields
- Attosecond physics

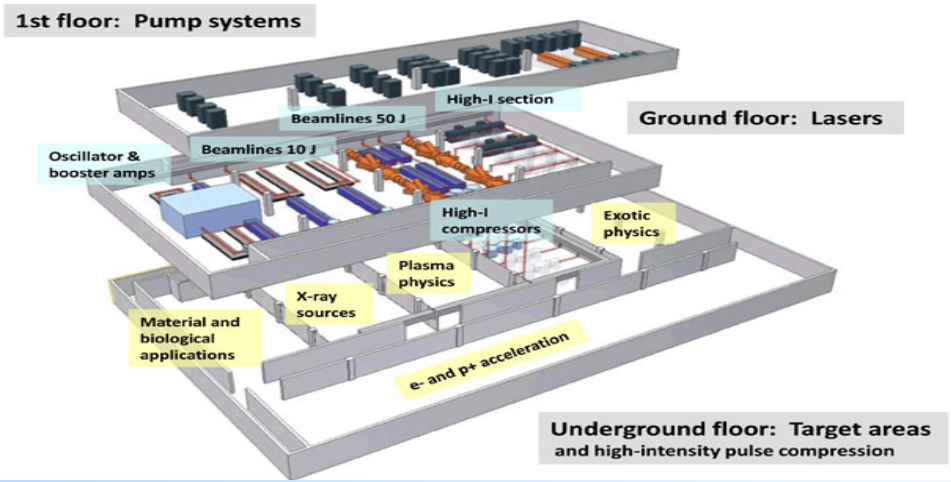

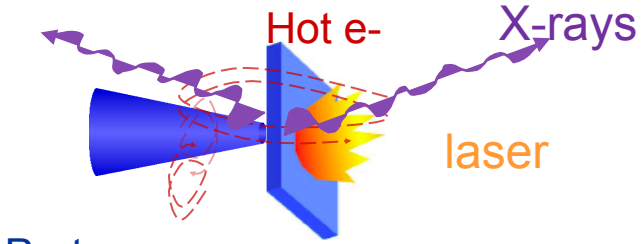

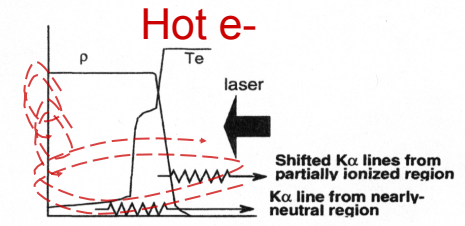

Z Pinches

Z machine at Sandia creates ~ 2 MJ, 15TW of x-rays from 27 million Amperes

Cylindrical wire array

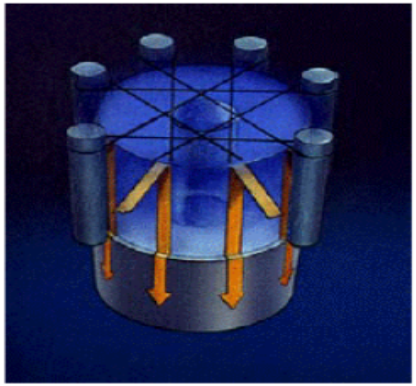

Inward J X B force

Implosion

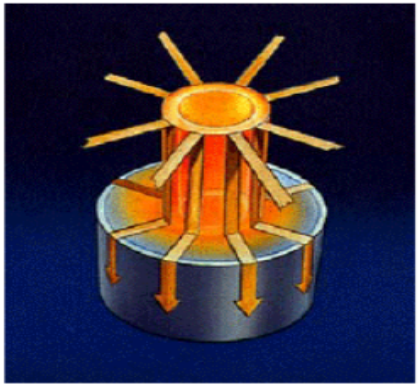

Inward acceleration

Stagnation

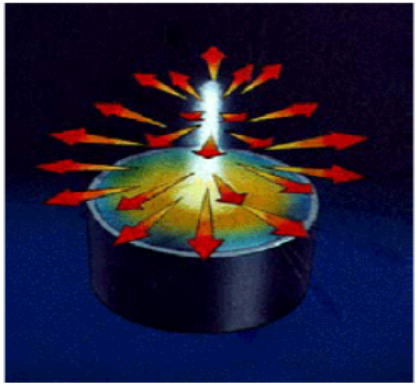

Shock heating &
Radiative cooling

X-ray Free

- Ultrashort pulses
- High photon energ
- High photon numb

olutions

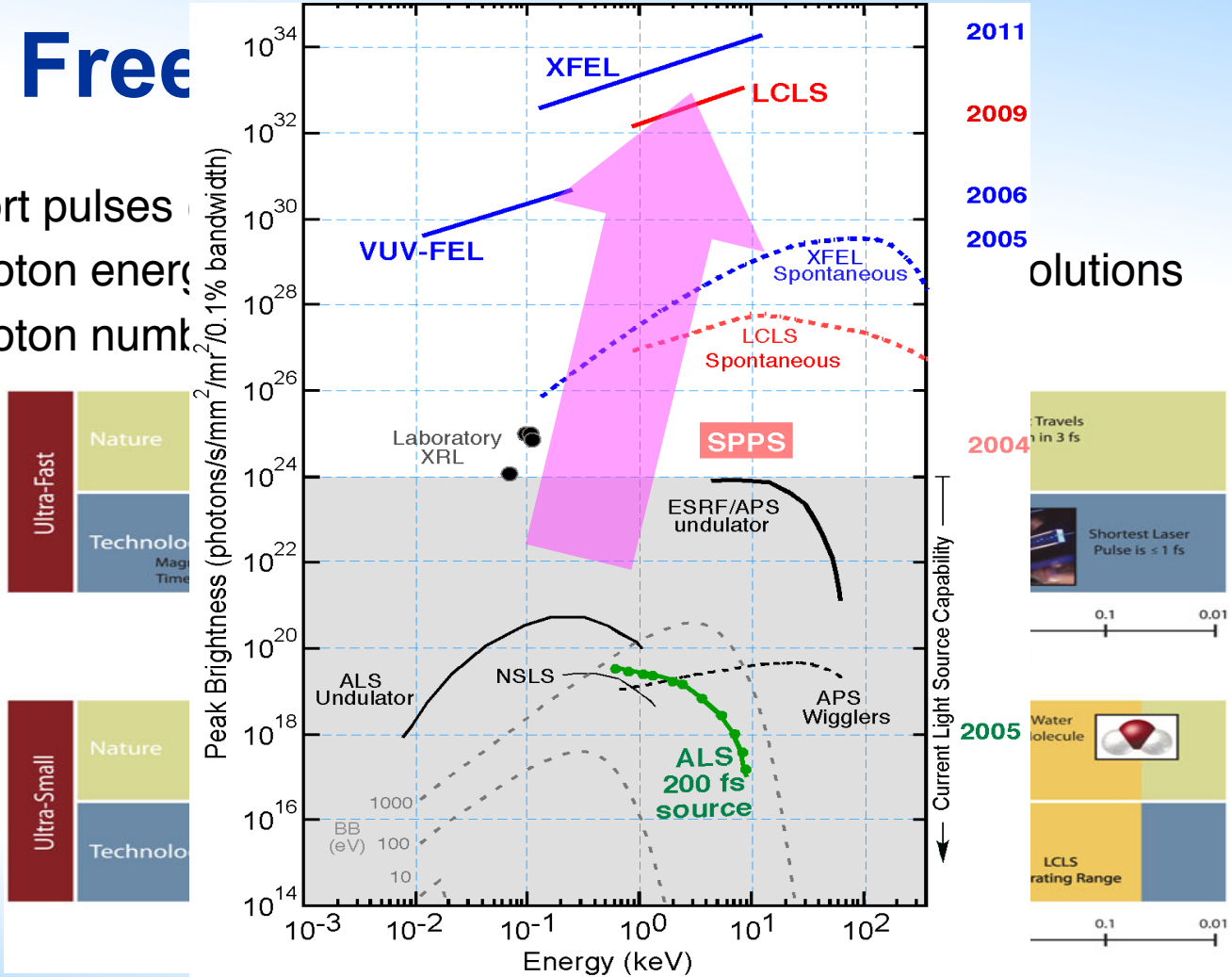

DENSE PLASMAS GENERATED BY X-RAY FREE ELECTRON LASERS

XFEL: Intense, short pulse, tunable sources to probe into the matter under extreme conditions

❖ High photon energy (500-20000 eV)

- heat the solid target volumetrically and generate quasi-uniform plasma

❖ Ultrashort pulses (2-340 fs)

- little hydrodynamic motion during the pulse minimize gradients to create a uniform, finite-temperature, solid-density plasma
- K-shell spectra dominated by the atomic states during the laser pulse

❖ High photon number (10^{12} photons or 10^{5} x-rays/Å^{2})

- Collision-dominated solid density plasma generated by the complex atomic processes driven by photo-ionization and Auger decay and later by collisions.

Spectroscopic observation of XFEL produced plasmas provide a unique opportunity to “see” the electron density of states of a finite temperature solid-density plasma

XFEL heats up plasmas up to 200 eV

Creation and diagnosis of solid-density hot-dense matter with an XFEL, S. Vinko, Nature 482, 59 (2012)

Detailed model for hot-dense aluminum plasmas generated by an XFEL, Ciricosta, PoP, 23, 022707 (2016)

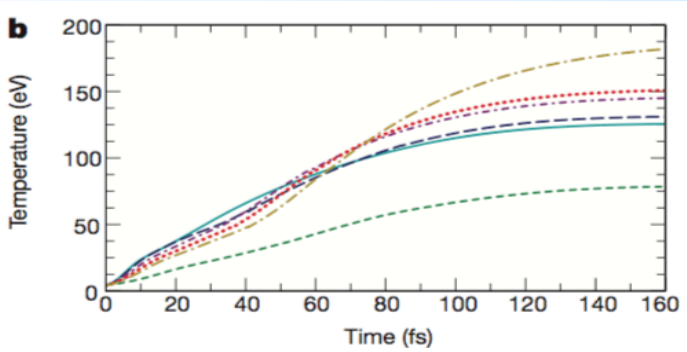

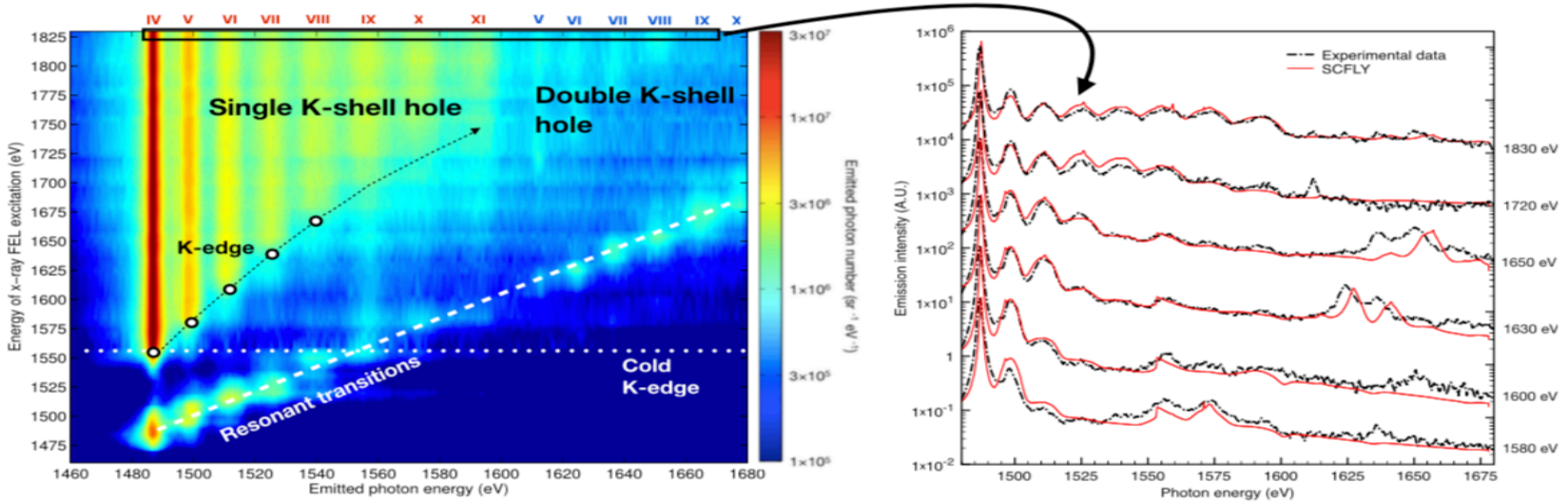

Observed spectra is time-integrated with contributions from different charge states

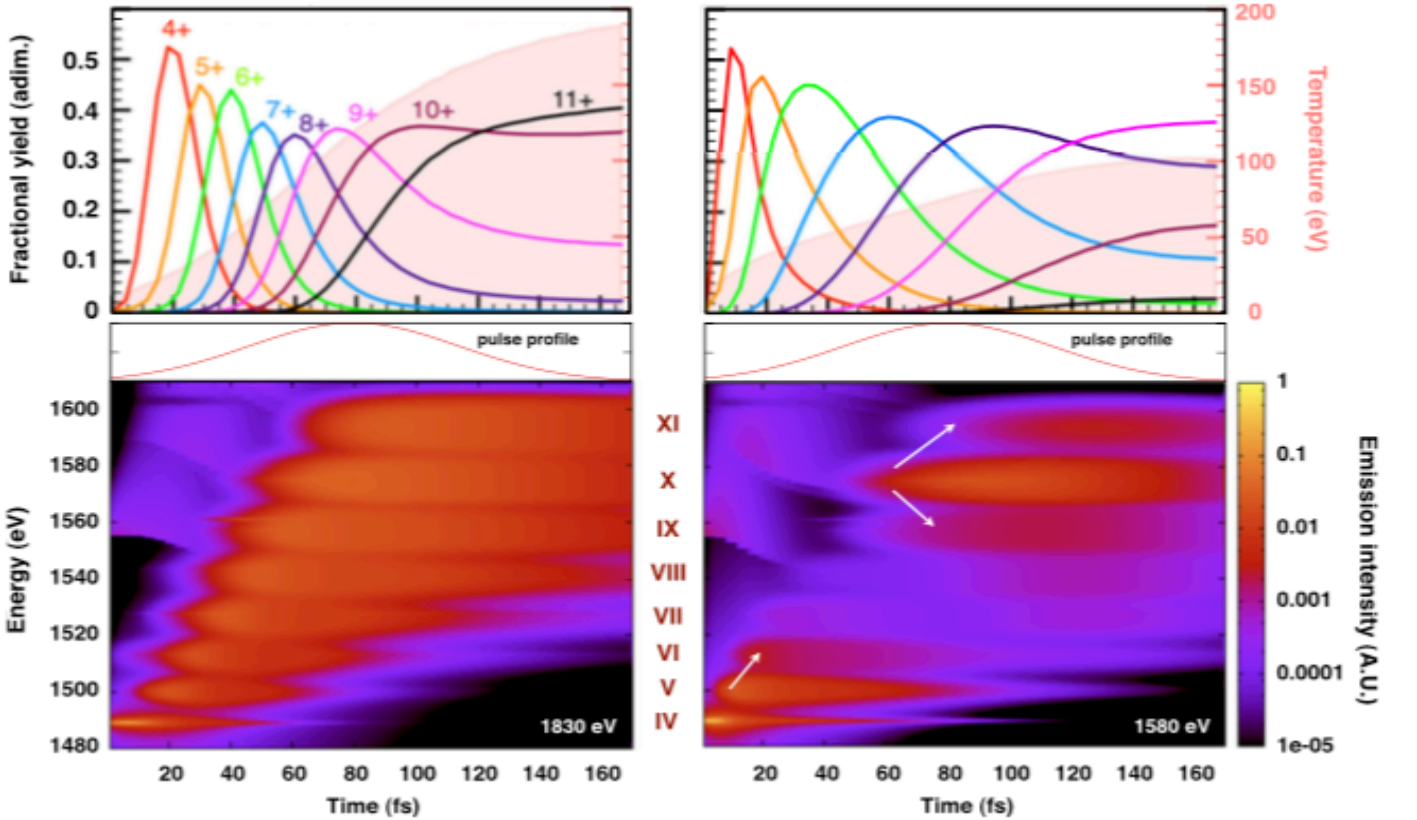

Hot, dense plasma generated by photoionization, Auger decay and collisional ionization

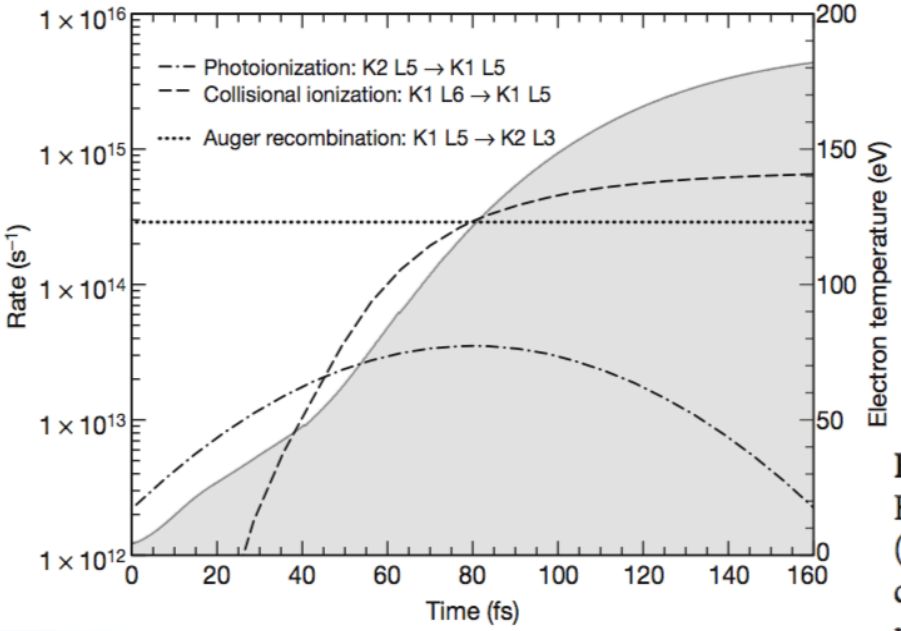

Figure 4 | Rates for atomic and collisional processes. Comparison between K-shell photoionization, collisional ionization and Auger recombination rates (broken curves, left-hand vertical axis) involved in populating and depopulating charge state VII at an X-ray photon energy of 1,830 eV. This state is one of the most populated for conditions leading to a peak temperature of ~100 eV. The calculation is conducted with a Gaussian beam (80 fs FWHM) centred at 80 fs. The electron temperature is given by the solid curve with grey shading under (right-hand vertical axis). By the peak of the pulse at 80 fs, the collisional ionization rate exceeds all others, dominating the population dynamics.

Spectroscopic observations reveal atomic structures and processes in a plasma

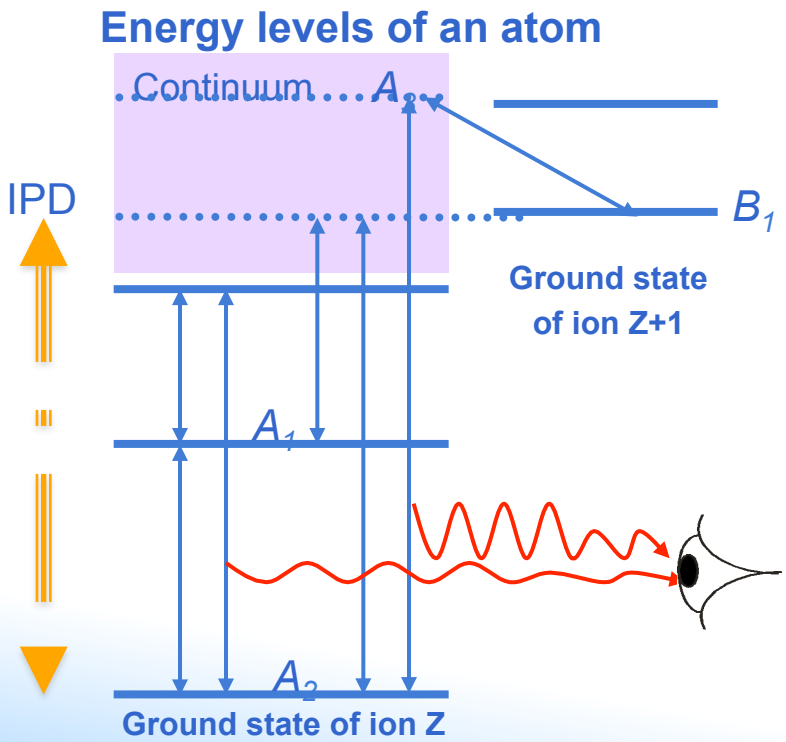

BOUND-BOUND TRANSITIONS

$A_1 \rightarrow A_2 + h\nu_2$ Spontaneous emission

$A_1 + h\nu_1 \leftrightarrow A_2 + h\nu_1 + h\nu_2$ Photo-absorption or emission

$A_1 + e_1 \leftrightarrow A_2 + e_2$ Collisional excitation or deexcitation

BOUND-FREE TRANSITIONS

$B_1 + e \rightarrow A_2 + h\nu_3$ Radiative recombination

$B_1 + e \leftrightarrow A_2 + h\nu_3$ Photoionization / stimulated recombination

$B_1 + e_1 \leftrightarrow A_2 + e_2$ Collisional ionization / recombination

$B_1 + e_1 \leftrightarrow A_3 \leftrightarrow A_2 + h\nu_3$ Dielectronic recombination

(autoionization + electron capture)

Ionization Potential Depression is critical to explain spectral features of dense plasmas

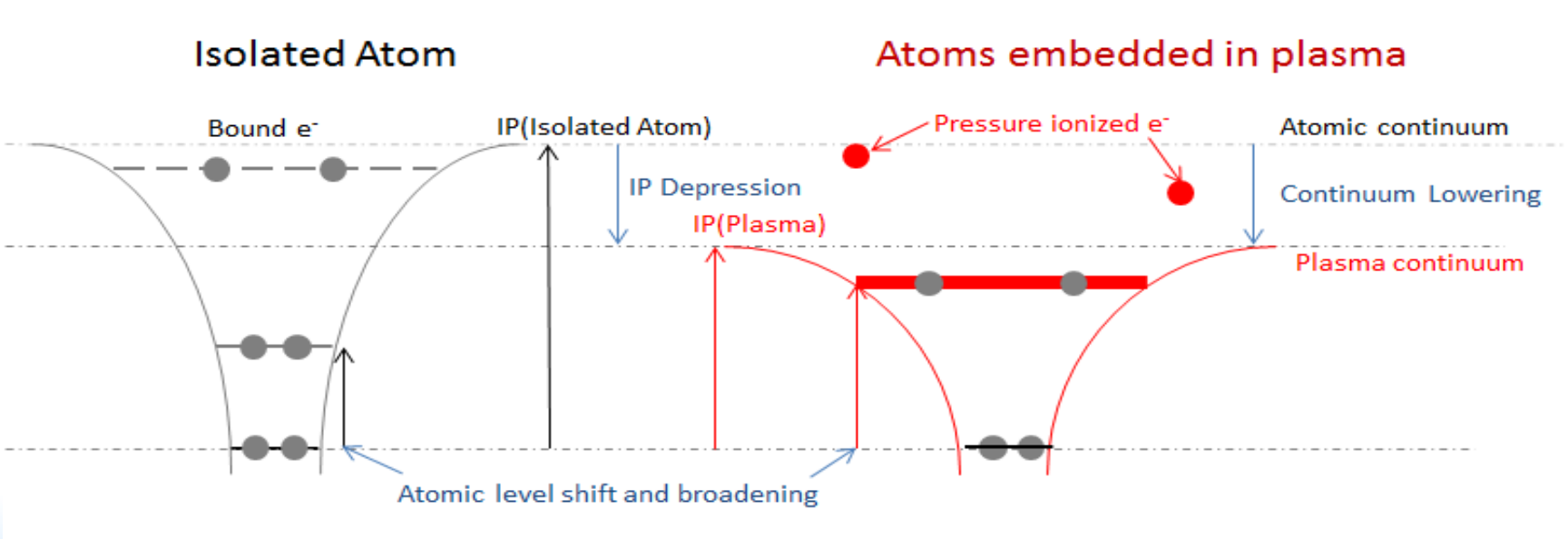

Radiation intensity is a function of atomic state population distributions

- Radiation intensity ***I(r,n,ν,t)*** is determined self-consistently from the coupled integro-differential radiation transport and population kinetic equations

$$[c^{-1}(\partial/\partial t) + (\mathbf{n}\cdot\nabla)]I(\mathbf{r},\mathbf{n},\nu,t) = \eta(\mathbf{r},\mathbf{n},\nu,t) - \chi(\mathbf{r},\mathbf{n},\nu,t)I(\mathbf{r},\mathbf{n},\nu,t)$$

- Opacity $\chi(\mathbf{r},\mathbf{n},\nu,t)$ and emissivity $\eta(\mathbf{r},\mathbf{n},\nu,t)$ are obtained with population densities and radiative transition probabilities

$$\chi_\nu = \sum_i \sum_{j>i} [n_i - (g_i/g_j)n_j]\alpha_{ij}(\nu) + \sum_i (n_i - n_i^* e^{-h\nu/kT})\alpha_{i\kappa}(\nu) + \sum_\kappa n_e n_\kappa \alpha_{\kappa\kappa}(\nu,T)(1-e^{-h\nu/kT})$$

$$\eta_\nu = (2h\nu^3/c^2)\left[\sum_i \sum_{j>i} (g_i/g_j)n_j\alpha_{ij}(\nu) + \sum_i n_i^* e^{-h\nu/kT}\alpha_{i\kappa}(\nu) + \sum_\kappa n_e n_\kappa \alpha_{\kappa\kappa}(\nu,T)e^{-h\nu/kT}\right]$$

O. Ciricosta, Physical Review Letters, 109, 065002 (2012)
Direct Measurements of the IPD in a Dense Plasma
S. Vinko, Nature Communications 5, 3533 (2014).
Density functional theory calculations of continuum lowering in strongly coupled plasmas.
S. Vinko, Journal of Plasma Physics. 81, 365810501 (2015)
X-ray free-electron laser studies of dense plasmas
O. Ciricosta, Nature Communications, (2016)
Measurements of continuum lowering in solid-density plasmas created from elements and compounds

DIRECT MEASUREMENTS OF THE IPD IN A DENSE PLASMA

Pressure ionization / Ionization Potential Depression of HED matter

- For dense plasmas, high-lying states are no longer bound due to interactions with neighbouring atoms and ions leading to a “pressure ionization”
- Ionization potentials are a function of plasma conditions

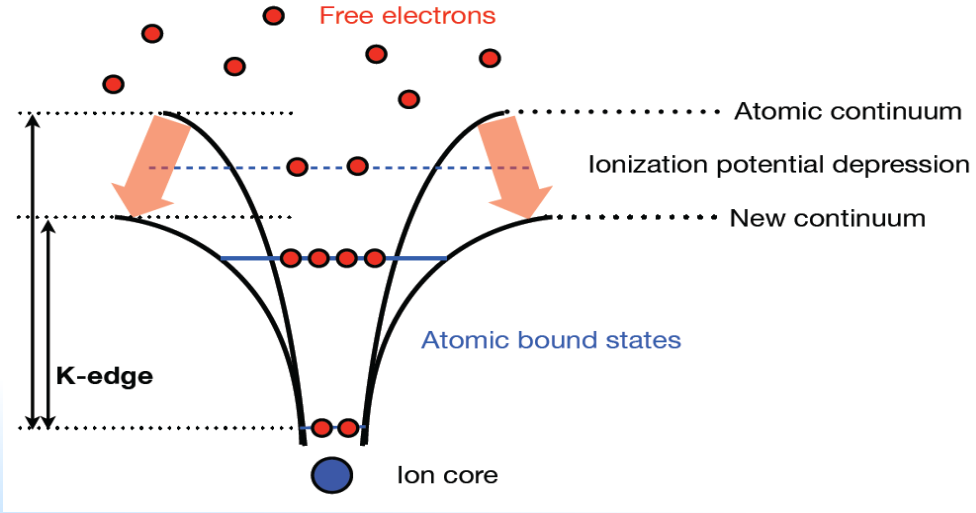

How is K_α emission created by XFEL?
How is it related to K-edge measurements?

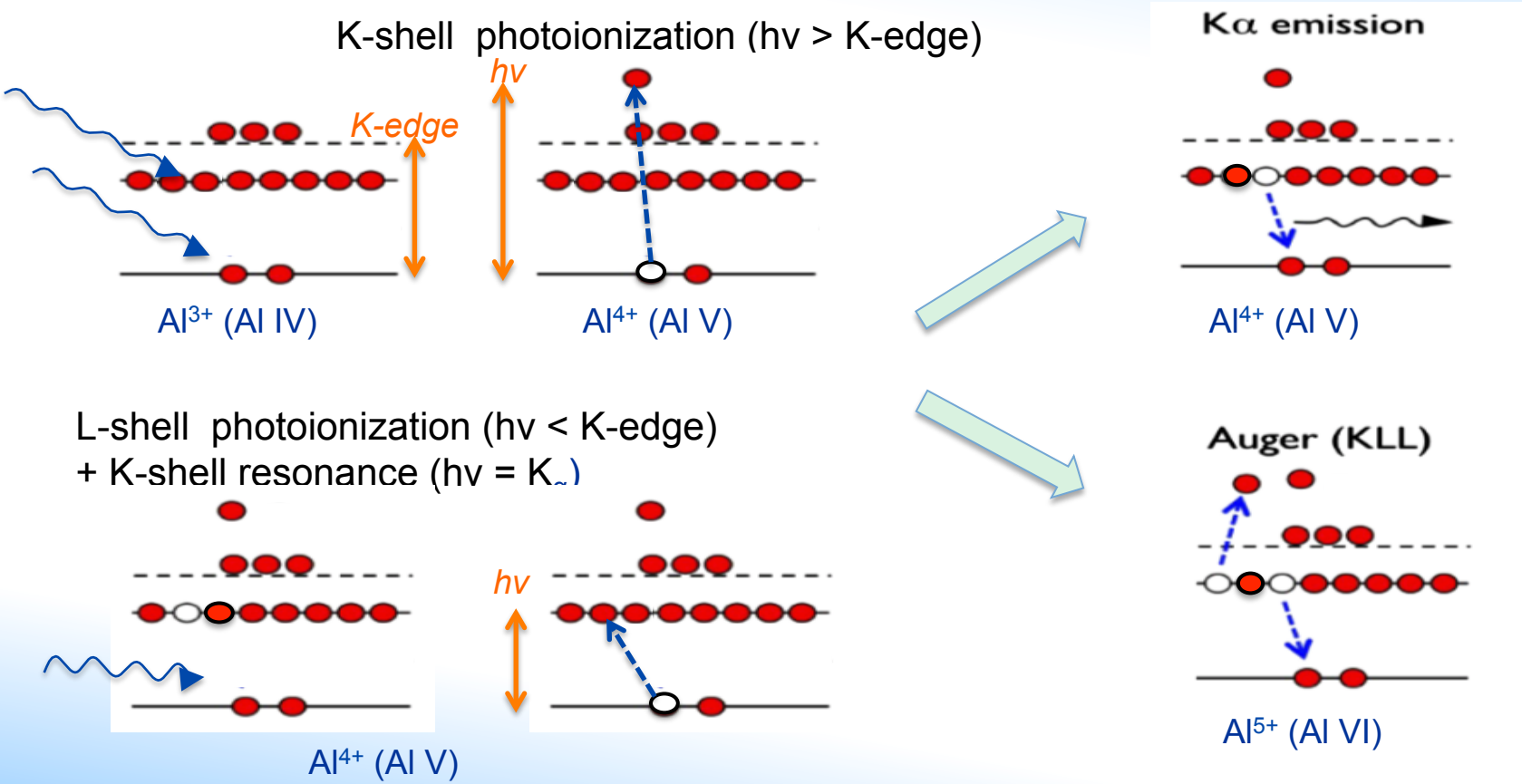

K-edge energies of Al IV-XI in solid-density plasmas are determined experimentally

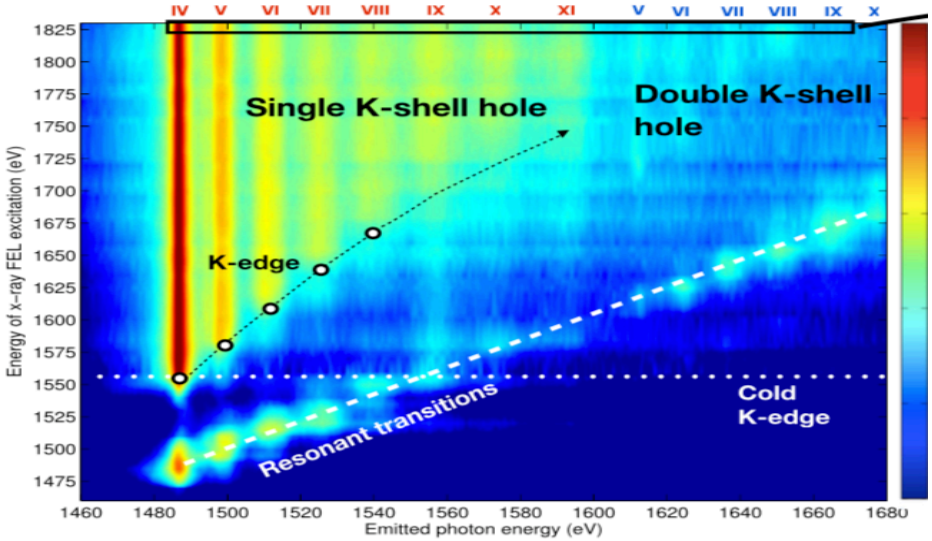

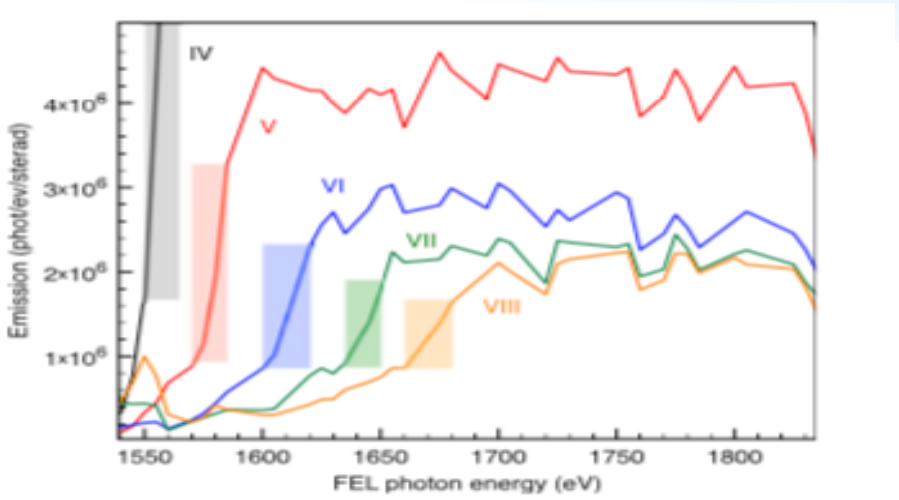

FIG. 7. Measured emission thresholds for lines VI-VIII. The curves can be obtained from the color-encoded plot in Fig. 1, by taking vertical lineouts for each of the emission lines. The shaded regions correspond to the K-edge regions as quoted on the continuum lowering paper.[8]

O. Ciricosta, Physics of Plasmas 23, 022707 (2016)
Detailed model for hot-dense aluminum plasmas generated by an x-ray free electron laser

Observed K-edges are much smaller than the atomic K-edge

- A new Ecker-Kroll (EK) model works better than Stewart-Pyatt (SP) model with higher IPD energy and hence unbound M-shell electrons

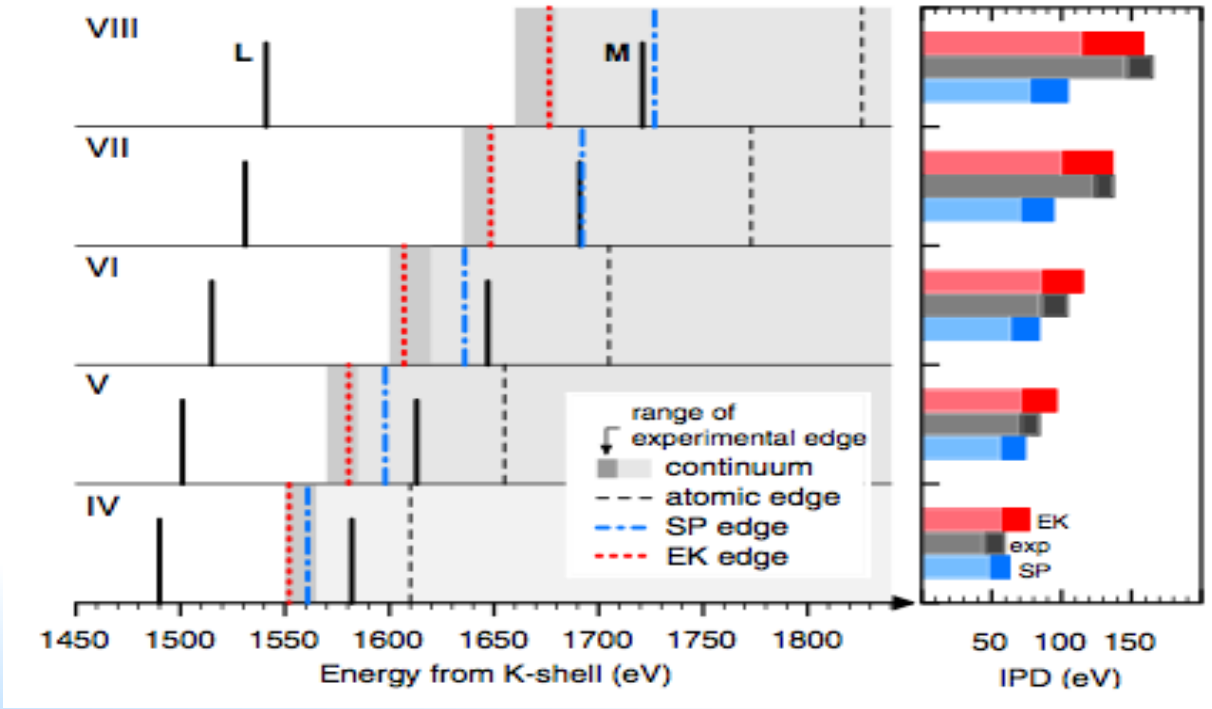

Stewart-Pyatt (SP) Model based on average plasma density has been used for 50+ years

- Reference: Lowering of ionization potentials in plasmas. Astrophys. J. 144, 1203–1211 (1966)
- When the plasma is quite dilute there will be a distance equal to the Debye length at which the states are no longer bound.

$$\Delta E \sim \frac{ze^2}{r_d}$$

r_d is the Debye radius defined as

$$r_d = 743.4\sqrt{\frac{T_e}{N_e(1+\bar{Z})}} \quad \text{(cm)}$$

- When the plasma is dense the volume per ion will be reduced to the point where significant overlap of the wave functions of the higher-lying states occurs. The orbital electrons in those states are essentially free.

$$\Delta E \sim \frac{ze^2}{r_i}$$

r_i is the ion sphere radius defined as

$$r_i = \left[0.75\frac{\bar{Z}}{N_e}\right]^{1/3} \quad \text{(cm)}$$

- Analytic expression based on Thomas-Fermi potential

$$\Delta E = 2.16\text{x}10^{-7}\,\frac{z}{r_i}\left(\left(1+\left(\frac{r_d}{r_i}\right)^3\right)^{2/3} - \left(\frac{r_d}{r_i}\right)^2\right)$$

Spectral features also reveal IPD effects

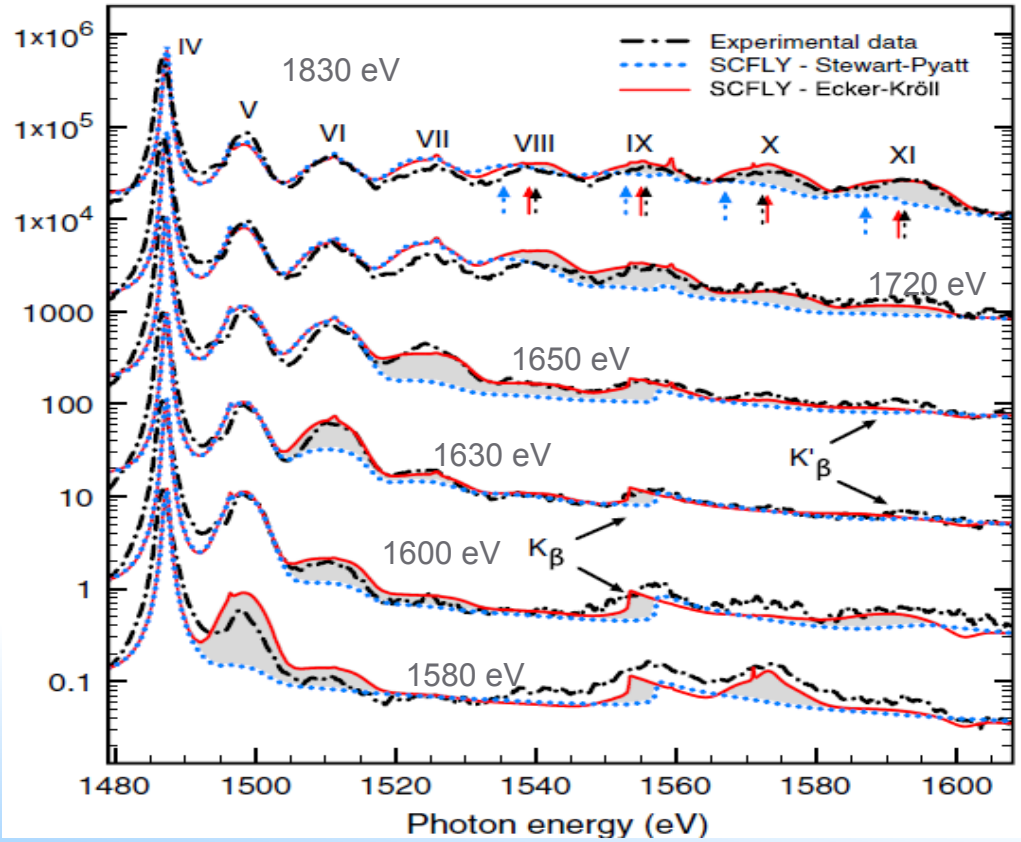

PRL 109, 065002 (2012)

SP model challenged after more than 50 years of extensive uses in astrophysics, cosmology, planetary science and inertial confinement fusion research.

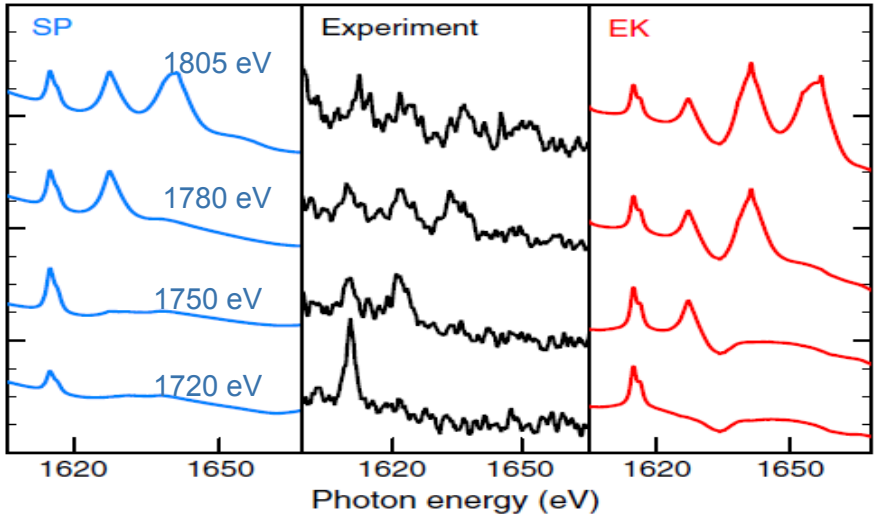

Most IPD models disagree with measured IPD of solid-density aluminum plasma

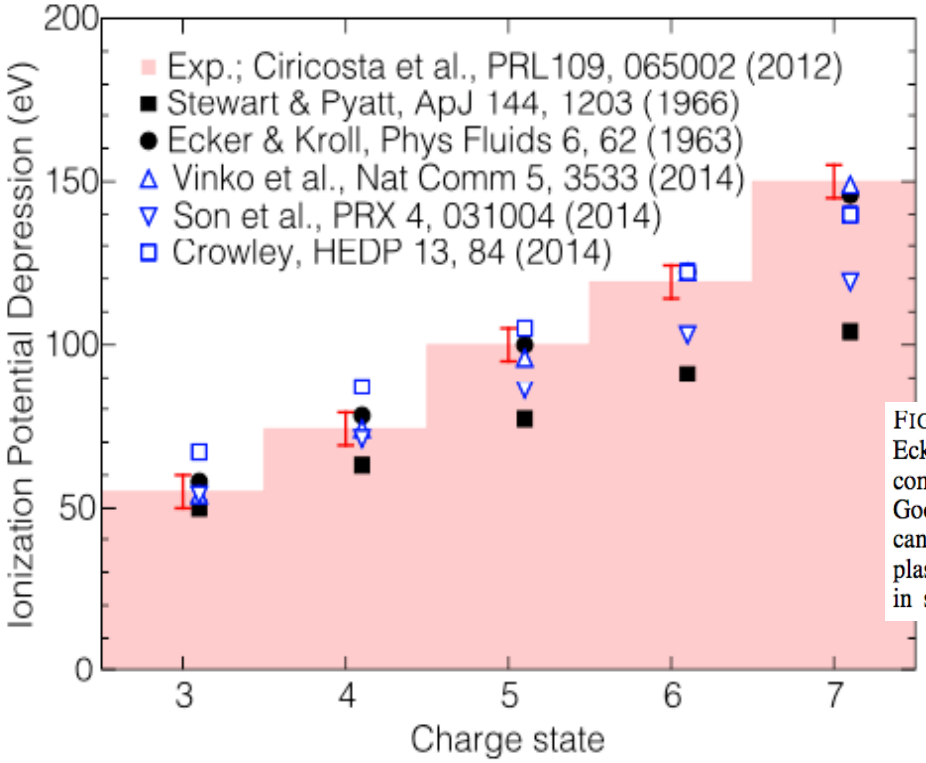

FIGURE 4. Comparison of IPD models. The IPD models of Stewart & Pyatt (1966), Ecker & Kröll (1963), Crowley (2014), Son *et al.* (2014) and Vinko *et al.* (2014) are compared with the experimental results by Ciricosta *et al.* (2012) obtained on the LCLS. Good agreement between all the models and the data within the experimental uncertainty can only really be found for the ground state (Al 3^+) even for the relatively simple Al plasma, exemplifying the current difficulties in the theoretical treatment of density effects in strongly coupled plasmas.

All IPD models based on average plasma density disagree with measured Al IPD

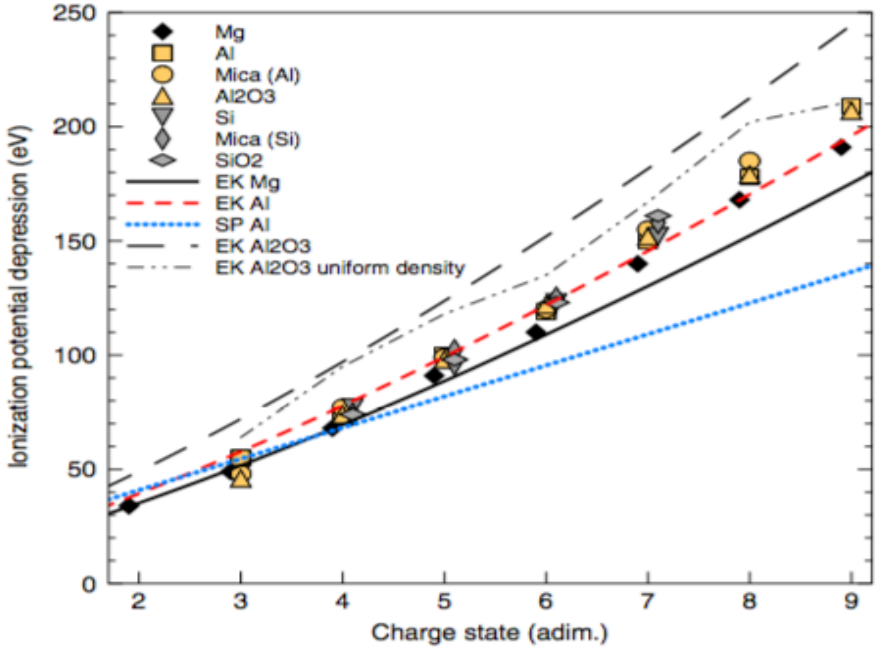

- For fixed average ionization and ion density n_i, EK and SP predict an IPD proportional to the inverse of the ion-sphere radius
- The ion densities in solid Al and Al_2O_3 are $6x10^{22}$ and $1.2x10^{23}cm^3$, respectively.
- However, the three data sets for Al and those for Si almost exactly overlap with each other, in stark contrast with the theoretical predictions.

Extreme care must then be taken when performing simulations of dense, ionized mixtures, which is of great importance in astrophysics and inertial-fusion science.

The measured K-edge energies agree well with DFT results

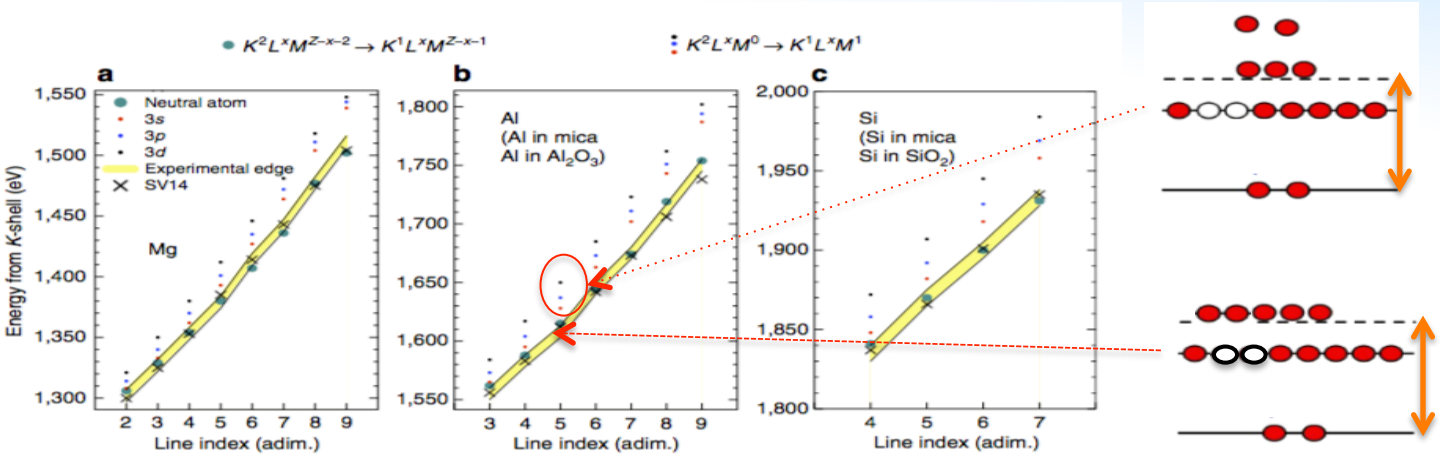

The measured K-edges are found to closely match the K–M excitation energies in neutral isolated atoms with the relevant number of L-shell holes.

For the cold solid-density materials, the ion density is fully determined by the atomic properties of the elements composing the crystal and the valence band can be approximated as originating from the overlap of free-atom orbitals from different sites, for both elements and mixtures.

Experimental results provide strong evidence that the same holds even for the hotter, highly ionized samples presented here, which is consistent with the largely temperature-independent valence density of states predicted by DFT results.

S. Vinko, Nature Communications, 6, 6397 (2015)

Investigation of femtosecond collisional ionization rates in a solid-density aluminium plasma

Q. Van der Berg, PRL, 120, 055002 (2018)

Clocking Femtosecond Collisional Dynamics via Resonant X-Ray Spectroscopy

MEASUREMENTS OF COLLISIONAL IONIZATION RATES AT SOLID DENSITY

What results K_α emission in the Red Box?

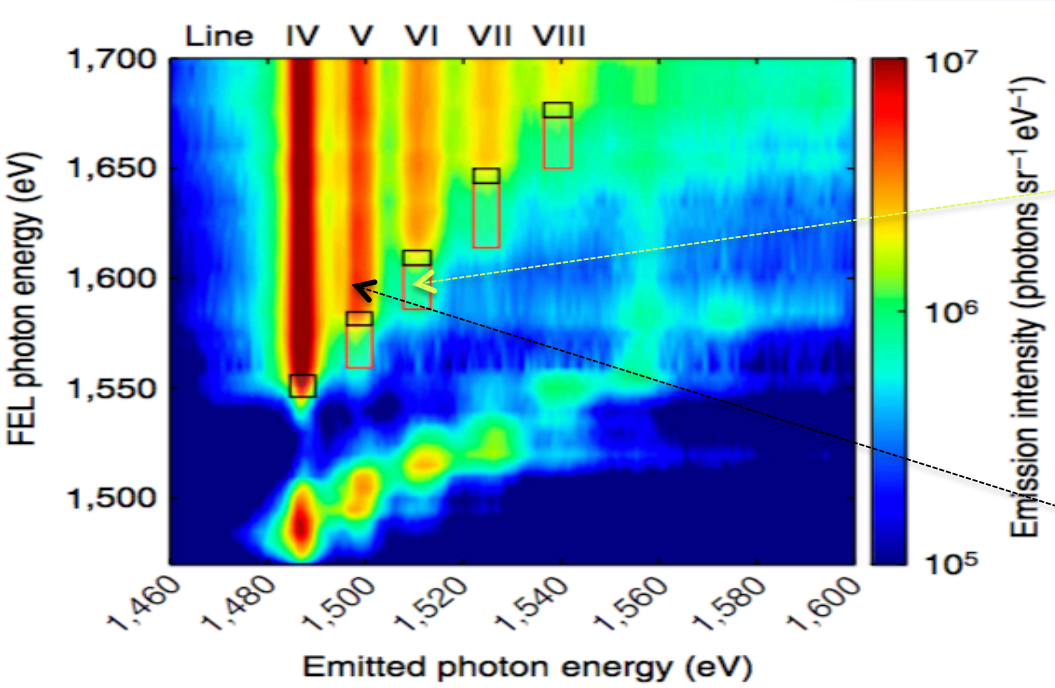

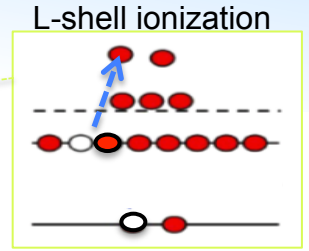

Al^{5+} (Al VI)

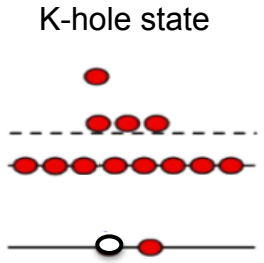

Al^{4+} (Al V)

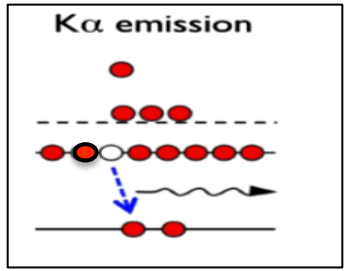

Al^{4+} (Al V)

- Black Box: K-edge energies
- Red Box: Collisional ionization from L-shell

Charge state distributions dominated by collisional ionization processes

What is a collisional ionization rate in a strongly-coupled, warm dense plasma?

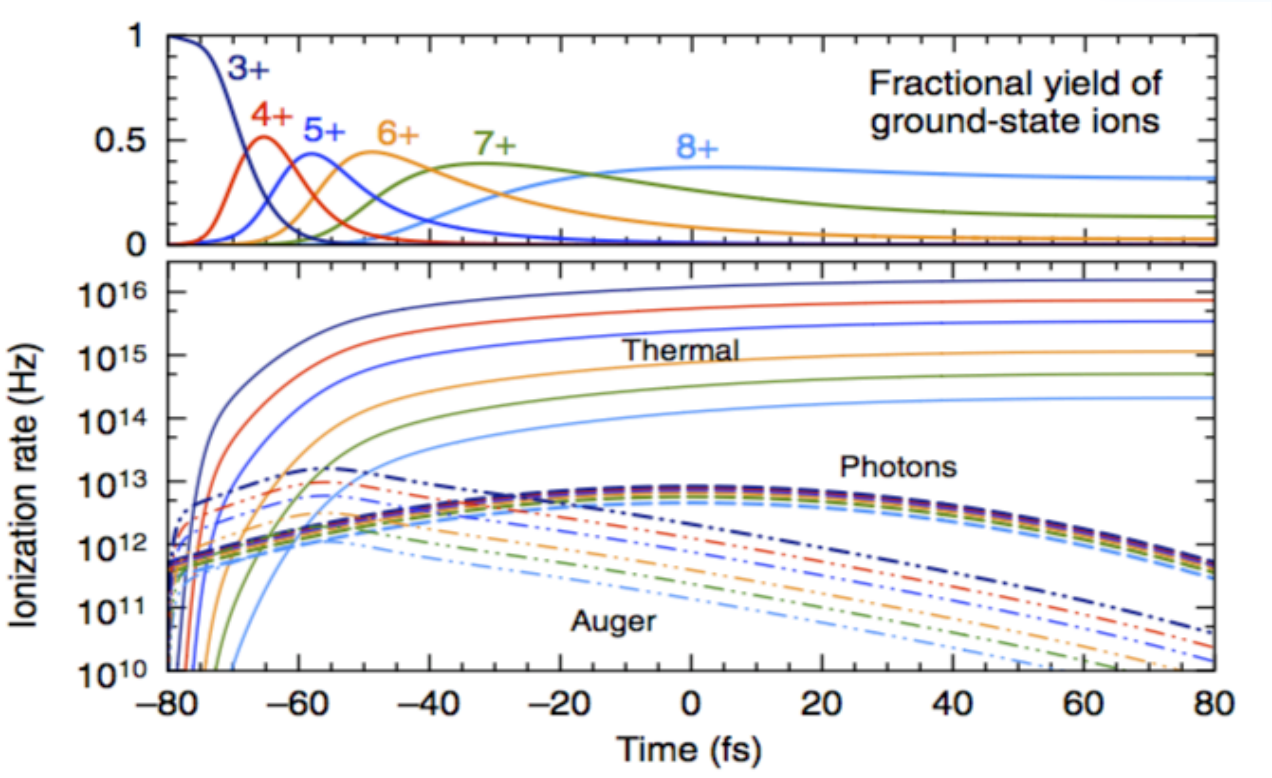

Core-hole pumping creates Mg K_α lines by L-shell ionization and K-shell photoexcitation

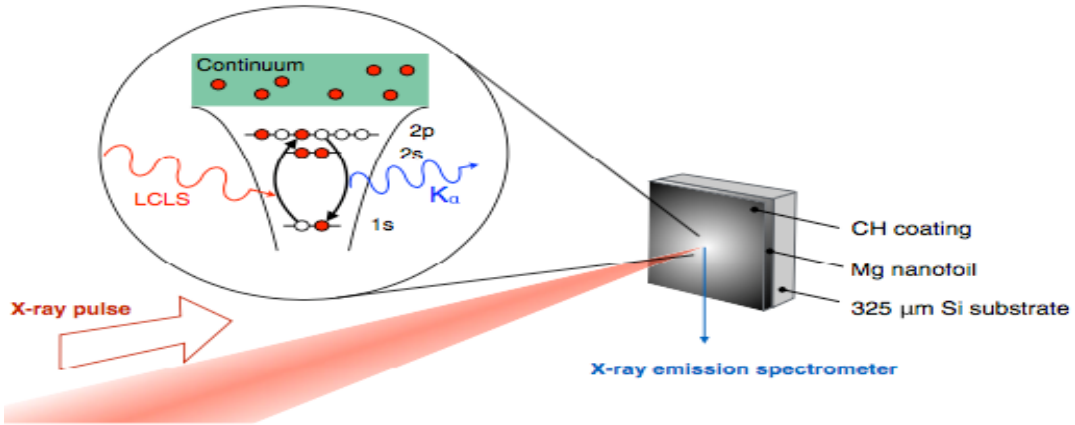

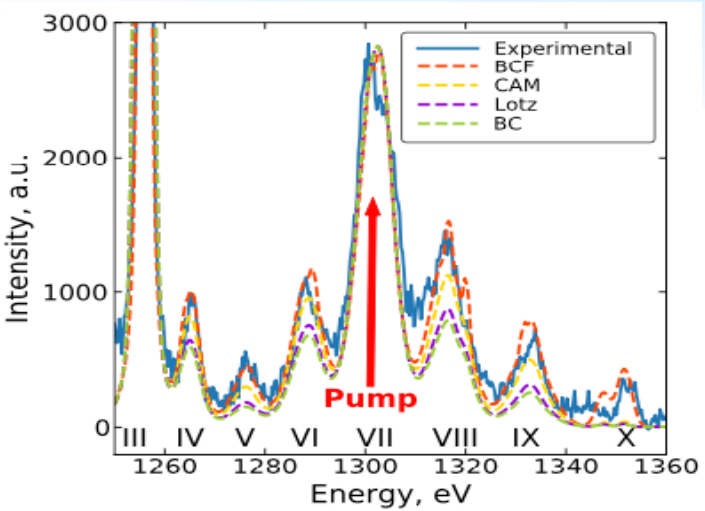

- The main peak Mg^{7+} is driven by XFEL pumping of $K^2L^3 \rightarrow K^1L^4$
- Other peaks are produced by ionization from K^1L^4 to K^1L^3 or by recombination to K^1L^5 .
- L-shell photoionization rates are much smaller than collisional ionization rates.
- The collisional ionization time scale is comparable to Auger time scale.

Density scaling due to IPD should be revisited.

- Generally, a density scaling is implemented by applying a reduced ionization potential in cross-section expressions.
- Collisional ionizations should no longer be considered binary events at high densities but become increasingly many-body screened interactions
- The density scaling proposed by Fontes, Sampson, and Zhang agrees with experiments. Phys. Rev. A 48, 1975 (1993)

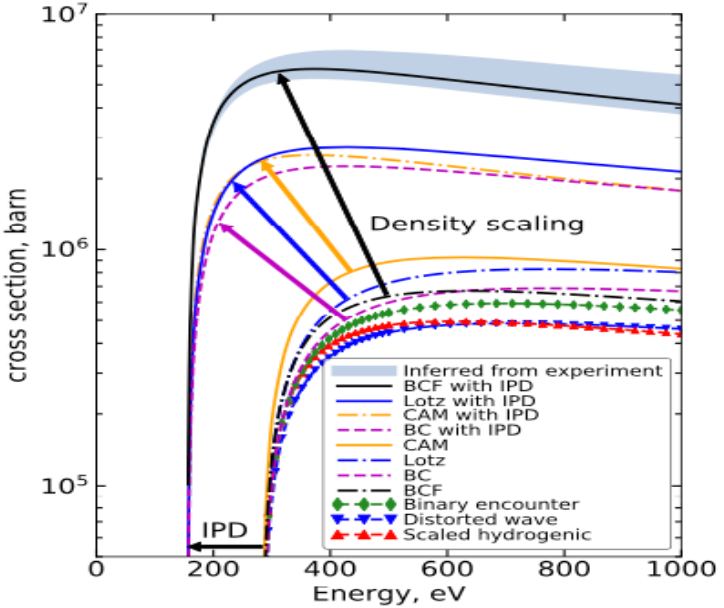

$$\sigma_{\mathrm{BCF}}(\varepsilon) = \frac{\pi a_0^2}{(I_i/I_H)^2}\frac{\zeta_i}{R_0^4}\frac{I_i'}{\varepsilon}\left\{\left(c_1 + \frac{c_2 + c_3 l}{n}\right)\log\left(\varepsilon/I_i'\right) + R_0\left(c_4 + \frac{c_5 + c_6 l}{n}\right)\left(1 - \frac{I_i'}{\varepsilon}\right) + R_0^{r_n}\left(c_7 + \frac{c_8 + c_9 l}{n}\right)\left(1 - \frac{I_i'}{\varepsilon}\right)^2\right\},$$

Concluding Remarks

- Interesting states of matter at extreme conditions are created in laboratory to study High Energy Density Physics and dense plasmas.
- XFEL provides a unique opportunity to probe into the electronic structures of finite temperature dense matter with spectroscopic measurements.
- Continuum lowering and ionization potential depression play a critical role in determining charge state distributions, average mean charge, equation of states and opacity, all relevant to thermodynamic properties of a plasma in HEDP.
- Electronic structures and collisional cross-sections of finite temperature dense plasmas are not well known.
- More theoretical and experimental work are needed.